

Received 16 June 2025; revised 30 July 2025; accepted 11 August 2025. Date of publication 15 August 2025; date of current version 2 September 2025.

Digital Object Identifier 10.1109/OJCOMS.2025.3599476

Adaptive Beam Pairing and Local Interpolation for Robust Analytical Beam Training in RIS-Assisted Wideband THz Systems

ZAID ALBATAINEH^{ID 1} (Senior Member, IEEE), HAYTHEM BANY SALAMEH^{ID 2} (Senior Member, IEEE), MOHAMMAD AL BATAINEH^{ID 3}, AND AHMED MUSA ALSHORMAN⁴

¹ Electronics Engineering Department, Yarmouk University, Irbid 21163, Jordan

² College of Engineering, Al Ain University, Al Ain, UAE

³ Electrical and Communication Engineering Department, United Arab Emirates University, Al Ain, UAE

⁴ Telecommunications Engineering Department, Yarmouk University, Irbid 21163, Jordan

CORRESPONDING AUTHOR: M. A. BATAINEH (e-mail: mffbataineh@uaeu.ac.ae)

This work was supported by the United Arab Emirates University (UAEU).

ABSTRACT Wideband terahertz (THz) communication systems offer ultra-high data rates and low latency for future sixth-generation (6G) networks, but they face severe path loss and beam split effects that degrade direction estimation in reconfigurable intelligent surface (RIS)-assisted deployments. Accurate beam training in these systems is particularly challenging under coarse codebooks and low signal-to-noise ratio (SNR) conditions. To overcome these limitations, we propose a robust analytical beam training framework, termed WBPC-AI, which integrates two key enhancements. First, a Weighted Beam Pair Combination (WBPC) mechanism aggregates information from the top k beam pairs using SNR-aware weighting, improving the stability of the estimation under noise and quantization. Second, an Adaptive Interpolation (AI) step refines direction estimates to sub-codebook resolution by exploiting parametric power asymmetries between neighboring beams. The proposed method avoids the drawbacks of hard decision-based schemes while maintaining low complexity. Simulation results demonstrate that WBPC-AI outperforms conventional analytical, hierarchical, and narrow-beam exhaustive search baselines in both angle estimation accuracy and achievable rate, particularly in low-SNR and large-RIS scenarios. Moreover, WBPC-AI exhibits strong scalability across RIS configurations and robustness under quantized phase control, validating its suitability for real-time RIS-assisted wideband THz systems.

INDEX TERMS Terahertz (THz), sixth-generation (6G), line-of-sight (LoS), reconfigurable intelligent surfaces (RIS), beamforming.

I. INTRODUCTION

TERAHERTZ (THz) communication is envisioned as a key enabler of sixth-generation (6G) wireless networks. It offers abundant spectral resources crucial for achieving ultra-high data rates with minimal latency, while supporting massive device connectivity required for diverse applications and services, including advanced mobile broadband, Internet of Things (IoT) connectivity, and enhanced virtual and augmented reality experiences [1]. However, the large-scale deployment of THz communication faces several deployment challenges, including severe path loss, which can significantly diminish signal strength over relatively short

distances, and molecular absorption, where the presence of atmospheric gases can absorb some of the transmitted THz signals, leading to further degradation of communication quality. In addition, this frequency band is highly susceptible to physical obstructions, making it difficult to maintain reliable communication links, especially when the direct line-of-sight (LoS) path is blocked [2]. To address these challenges and enhance communication reliability, reconfigurable intelligent surfaces (RIS) have emerged as a promising solution. RIS can dynamically control the reflection and direction of THz signals, enabling the formation of highly directional beams. This capability allows for establishing

additional reflective paths, often called virtual LoS, which can bypass obstacles without the need for extensive infrastructure changes or the deployment of additional active radio frequency (RF) chains [3]. Beyond beam alignment, RIS-assisted systems also face challenges in resource allocation and power optimization, particularly in multi-user scenarios with non-orthogonal multiple access (NOMA) requirements [29].

Accurate beam alignment is crucial in RIS-assisted THz communication systems to maximize array gain, maintain robust connectivity, and combat weak propagation environments [4]. Often designed for narrowband systems, traditional beam training schemes rely on narrowband exhaustive or hierarchical searches over discrete Fourier transform (DFT)-based codebooks to estimate the optimal beam direction [13]. However, these conventional methods become increasingly inefficient and less effective in wideband THz systems due to the *beam split* effect, a phenomenon in which frequency-dependent phase mismatches in the RIS cause the beam direction to deviate across the various subcarriers. The beam split not only degrades angular resolution, but also substantially reduces the effectiveness and robustness of beamforming, particularly under low signal-to-noise ratio (SNR) conditions [14], [15]. To mitigate these limitations, various beam training strategies have been proposed. Hierarchical training schemes improve efficiency by progressively narrowing the search space but require frequent feedback and are less robust in multi-user or noisy environments. Multi-directional scanning methods reduce overhead by probing multiple directions simultaneously, but still suffer from limited angular resolution [9], [16]. Meanwhile, data-driven deep learning approaches reduce interaction overhead, but are highly dependent on training data and exhibit performance degradation under beam-split conditions [17], [20]. Some studies have explored compensatory signal processing and hardware improvements to address spatial wideband effects [21], [22], although these often add complexity.

Recently, analytical frameworks have emerged as promising solutions for wide-band beam training. In particular, the analytical power-difference profile (PDP)-based method proposed in [5] estimates the user's direction by leveraging the power distribution across subcarriers, achieving low training overhead and improved scalability. However, existing analytical approaches remain vulnerable to noise and often exhibit limited estimation precision under coarse codebooks. More critically, their reliance on hard decision beam selection, i.e., selecting a single dominant beam pair, makes them particularly sensitive to noise and misalignment. Motivated by these limitations, we propose an improved analytical beam training framework to enhance robustness, accuracy, and real-time applicability in RIS-assisted wideband THz systems while relaxing the hard-decision beam selection requirement. Specifically, the main contributions of this paper are summarized as follows:

TABLE 1. List of key notations.

Symbol	Description
M, N	Number of RIS elements along x- and y-axes
H	RIS-assisted wideband THz channel matrix
μ	Central angles of beam directions
θ_{est}	Estimated direction of arrival (DoA)
p_i	Received power of i -th beam pair
k	Number of top beam pairs selected in WBPC
B	Communication bandwidth
f_c	Carrier frequency
SNR	Signal-to-noise ratio
ζ	Power ratio metric used in analytical estimation
C	Beamforming codebook

- We introduce a *Weighted Beam Pair Combination* (WBPC) mechanism with adaptive top- k selection based on SNR, enabling the integration of multiple high-energy beam measurements to mitigate the impact of noise and outliers.
- We propose a *local interpolation technique* to achieve sub-codebook angular resolution, refining beam direction estimates beyond the granularity of predefined codebooks and enhancing angular precision.
- We design both WBPC and local interpolation techniques to incur minimal computational overhead and require no additional hardware modifications, ensuring the practicality of the proposed framework for real-time deployment.
- We demonstrate through extensive simulations that the proposed framework outperforms existing analytical, hierarchical, and narrow-beam exhaustive search methods, particularly under low-SNR conditions and coarse codebook regimes, while maintaining scalability to multi-user and various RIS array configurations.

The remainder of this paper is organized as follows. Section II provides a detailed review of related work, highlighting recent advances and key challenges in beam training for RIS-assisted THz systems. Section III describes the system and channel model considered in this work. Section V presents the proposed Weighted Beam Pair Combination with Adaptive Interpolation (WBPC-AI) method. Section VI discusses simulation results and performance evaluation in various system scenarios. Finally, Section VII concludes the paper and outlines potential directions for future research.

Notations: Throughout this paper, we use the following notations: lowercase letters (e.g., x) represent scalars; bold lowercase letters (e.g., \mathbf{x}) indicate vectors; and bold uppercase letters (e.g., \mathbf{X}) signify matrices. The superscripts are used as follows: $(\cdot)^*$ for complex conjugates, $(\cdot)^T$ for transposes, and $(\cdot)^H$ for Hermitian transposes. The notation $\mathbb{C}^{M \times N}$ denotes the space of complex-valued $M \times N$ matrices. The Euclidean norm of a vector is denoted by $\|\cdot\|$, and the expectation is represented by $\mathbb{E}\{\cdot\}$. For ease of reference, the key notation is summarized in Table 1.

II. RELATED WORK

Beam training is a fundamental task in RIS-assisted THz systems, especially under wideband conditions where the *beam-split* effect introduces angular misalignment across subcarriers. This misalignment degrades the direction estimation accuracy and reduces the overall gain in beam formation.

Traditional beam training approaches, such as exhaustive DFT codebook searches [13], are accurate but incur high training overhead. Hierarchical search methods [14], [15] improve efficiency by iteratively narrowing the search space. However, they rely on frequent feedback and are less robust in dynamic or multi-user environments. To reduce training costs, multi-directional beam probing techniques [9], [16], [19] scan several directions simultaneously. Although more efficient, these methods suffer from limited angular resolution. Other works have addressed spatial-wideband effects by incorporating delay-phase compensation or beamspace processing [21], [22], though at the expense of increased signal processing complexity or hardware modifications.

Machine learning-based approaches, particularly deep neural networks (DNNs) [17], [18], [20], reduce the feedback burden and improve adaptability. However, their performance deteriorates under beam-split distortions and is highly dependent on the quality and diversity of training data. More recently, analytical beam training methods have gained attention for their ability to extract direction information from the frequency-domain characteristics of wideband THz channels. A notable example is the PDP-based method proposed in [5], which estimates direction-of-arrival (DoA) by exploiting the subcarrier power distribution profile. This approach significantly reduces training overhead and is scalable to large codebooks. However, it suffers from three key limitations:

- It employs *hard-decision beam selection*, relying solely on the most dominant beam pair, which makes it sensitive to noise and quantization.
- It is restricted to *coarse angular resolution* due to discrete codebook spacing.
- It lacks a mechanism to *fuse information across multiple candidate beams*, limiting robustness.

To overcome these issues, we propose an enhanced analytical framework that extends [5] with two new modules:

- 1) A *Weighted Beam Pair Combination with Adaptive selection* (WBPC-A), which aggregates top- k beam pairs using SNR-aware weighting to improve estimation stability and mitigate outliers.
- 2) A *local interpolation technique* that refines the estimated angle with sub-codebook resolution, improving angular precision without increasing complexity.

These enhancements maintain the low-complexity nature of the analytical framework while substantially improving robustness and accuracy in coarse-codebook and low-SNR scenarios. To better contextualize our contribution, Table 2 summarizes and compares the capabilities of representative

TABLE 2. Comparison of related beam training methods.

Method	Handles Beam Split	Low Overhead	Multi-user Ready	Fine Resolution
Exhaustive Search [13]	x	x	✓	✓
Hierarchical Search [14], [15]	x	✓	x	✓
Multi-directional [9], [16]	x	✓	✓	x
DNN-based [17], [20]	x	✓	✓	x
Analytical PDP [5]	✓	✓	✓	x
Proposed (WBPC-A + Interpolation)	✓	✓	✓	✓

beam training methods in RIS-assisted wideband THz systems. The comparison focuses on four key criteria: their ability to handle beam split effects, training overhead, suitability for multi-user scenarios, and angular resolution. As shown, while traditional and machine learning-based methods offer certain advantages, they often fail in at least one critical aspect. In contrast, the proposed framework, which incorporates WBPC-A and interpolation, provides a balanced solution that satisfies all four performance dimensions, demonstrating its suitability for practical wideband RIS deployments.

III. SYSTEM MODEL AND SPATIAL-WIDEBAND EFFECTS

We consider a downlink RIS-assisted wideband THz communication system employing orthogonal frequency division multiplexing (OFDM) with M subcarriers, as illustrated in Fig. 1. The system consists of a base station (BS), a reconfigurable RIS comprising N reflecting elements, and a user equipment (UE). The BS and UE are equipped with single antennas, while the RIS is modeled as a uniform linear array. Due to the severe path loss and blockage characteristics of the THz bands, we assume that the direct BS-UE link is blocked and that all communication is performed through the RIS [11].

The BS transmits with a total power budget P_t , and the transmit symbols are normalized so that $\mathbb{E}[|s_m|^2] = P_t$. The thermal noise at the UE receiver is modeled as $n_m \sim \mathcal{CN}(0, \sigma^2)$, where σ^2 is the noise variance. The channel fading coefficients $g_{\text{BR},m}$ and $g_{\text{RU},m}$ follow a frequency-selective Rician model with Rician factors K_{BR} and K_{RU} , respectively. The BS transmits OFDM symbols on M OFDM subcarriers with a total bandwidth B centered on frequency f_c . Let $f_m = f_c + \frac{B}{M}(m - \frac{M+1}{2})$ denote the frequency of the m -th subcarrier. The downlink LoS channel from the BS to the RIS on the m -th subcarrier can be modeled as follows:

$$\mathbf{h}_{\text{BR},m} = g_{\text{BR},m} e^{-j2\pi \tau_{\text{BR},m} f_m} \mathbf{a}_N(\phi_m), \quad (1)$$

where $g_{\text{BR},m}$ is the complex gain, ϕ_m denotes the frequency-dependent spatial angle, $\tau_{\text{BR},m}$ is the propagation delay, and $\mathbf{a}_N(\phi_m)$ is the RIS array response vector that is defined as:

$$\mathbf{a}_N(\phi_m) = \frac{1}{\sqrt{N}} \left[1, e^{j\pi\phi_m}, \dots, e^{j\pi(N-1)\phi_m} \right]^T. \quad (2)$$

Similarly, the channel from the RIS to the UE over subcarrier m can be modeled as follows:

$$\mathbf{h}_{\text{RU},m} = g_{\text{RU},m} e^{-j2\pi \tau_{\text{RU},m} f_m} \mathbf{a}_N(\psi_m), \quad (3)$$

where $\psi_m = \frac{2df_m}{c} \sin(\varsigma^{\text{AoA}})$ and ς^{AoA} denotes the angle of arrival (AoA) at the UE.

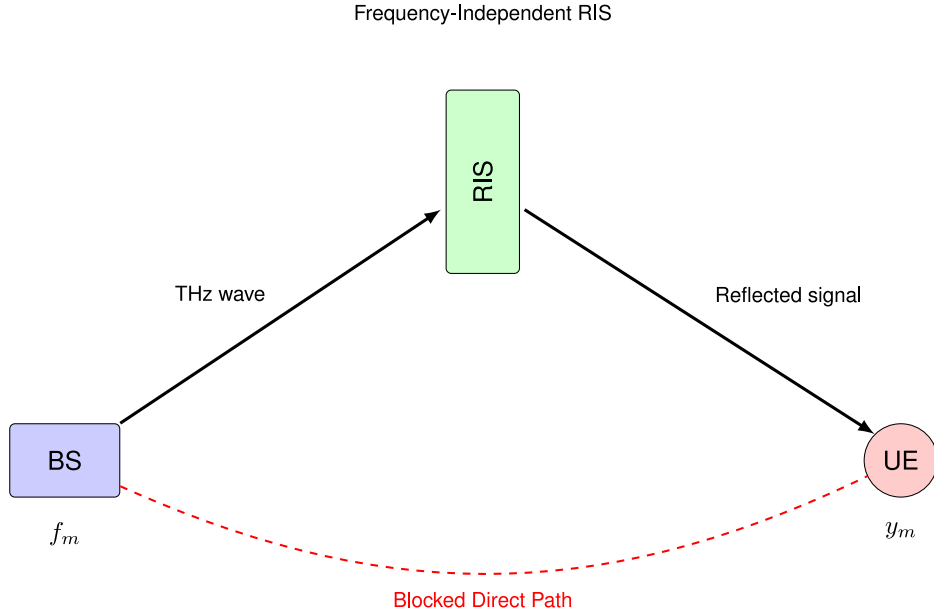


FIGURE 1. System model.

We assume a far-field planar wavefront, and elevation angle variation is neglected due to the assumed uniform user placement in the azimuthal plane, consistent with prior works that adopt Uniform Linear Arrays (ULAs) for RIS modeling in horizontally aligned deployments [23], [24], [25]. Although this simplification facilitates analytical tractability, its validity has been supported by comparisons with more comprehensive 2D planar array models that account for elevation in near-field and THz scenarios [26], [27], [28]. The RIS phase shift model is defined as $\phi_n = e^{j\theta_n}$, where θ_n is drawn from a quantized phase set determined by the controller's resolution (e.g., 1-bit, 2-bit, or 3-bit). This model captures the practical constraint of the granularity of finite phase control in hardware implementations of RIS. We also assume the RIS is passive and frequency-independent, i.e., the phase-shift matrix $\Theta = \text{diag}(e^{j\theta_1}, \dots, e^{j\theta_N})$ remains fixed across all subcarriers. This reflects practical implementations where fine-grained frequency-selective control is infeasible.

Given (1)-(3), the received signal at the UE over the m -th subcarrier can be expressed as follows:

$$y_m = \mathbf{h}_{\text{RU},m}^H \Theta \mathbf{h}_{\text{BR},m} s_m + n_m, \quad (4)$$

where s_m is the transmitted symbol, Θ represents the RIS phase-shift matrix, and n_m denotes the additive white Gaussian noise. While our analysis assumes a ULA and azimuth-only steering vector for simplicity, in Section VI, we extend the evaluation to uniform planar array (UPA) RIS configurations that account for azimuth and elevation angles.

For large RIS sizes (e.g., $N = 1024$ or 4096) and high frequencies (e.g., $f_c = 0.1$ THz), near-field propagation and mutual coupling effects may arise. These are not explicitly modeled in this work but are acknowledged as important

directions for future enhancement. Our model adopts the far-field planar assumption, commonly used in analytical beam training methods and consistent with prior work (e.g., [23], [24], [25], [26], [27], [28]), which is justified by typical deployment scenarios where the BS–RIS distance is much larger than the RIS aperture. However, when the user–RIS distance approaches or falls below the Rayleigh distance, the spherical nature of the wavefronts becomes significant, leading to beam pattern distortion and loss of steering vector orthogonality. Additionally, mutual coupling between RIS elements can alter the effective phase and amplitude responses, especially when inter-element spacing is sub-wavelength. Although our proposed WBPC-AI method is agnostic to the specific array geometry and operates in the angular domain, integrating electromagnetic effects such as near-field modeling and coupling compensation (e.g., via calibrated array manifolds) is a promising avenue for future work. We include this discussion to acknowledge the limitations of the current model and to motivate future enhancements using full-wave simulations or measurement-based validation in ultra-large and densely deployed RIS systems.

IV. BEAM TRAINING UNDER BEAM SPLIT PROBLEM IN RIS-ASSISTED WIDEBAND SYSTEMS

RIS enables THz communication by controlling signal propagation. However, a key challenge arises in wideband THz systems: the *beam split effect*. Unlike narrowband systems, where beam directions are nearly constant across subcarriers, wideband systems exhibit frequency-dependent beam directions, which complicates beam training and direction estimation. The following subsections examine the origin and impact of the beam split effect, formulate

the beam-training problem, and present existing analytical solutions.

A. BEAM SPLIT EFFECT IN WIDEBAND THZ SYSTEMS

The beam split effect arises from spatial-frequency coupling in wideband THz systems, where each subcarrier experiences a slightly different spatial propagation path. In narrowband systems, the spatial direction of a reflected beam remains approximately constant across frequencies. However, in wideband THz systems, even when the user is at a fixed angle, the spatial angle of the signal varies with frequency. This effect, known as the spatial wideband effect, causes beam misalignment across subcarriers and degrades the effectiveness of conventional beamforming. Specifically, the spatial angle for the m -th subcarrier is given by:

$$\phi_m = \frac{2df_m}{c} \sin(\varsigma), \quad (5)$$

where ς is the actual angle of the UE, d is the RIS element spacing, and c is the speed of light. Because a fixed RIS phase profile reflects each frequency differently, a frequency-independent RIS fails to align beams across all subcarriers. As a result, the reflected power spreads over multiple spatial directions, reducing the strength of the received signal and, consequently, the system's performance. Traditional beam training methods, which assume fixed beam directions across subcarriers, are ineffective in handling this dispersion.

B. PROBLEM STATEMENT AND MATHEMATICAL FORMULATION

The primary challenge in RIS-assisted wideband THz systems is to determine the UE's actual spatial direction ς that maximizes the received power at the UE despite the frequency-dependent spatial angles caused by the beam-split effect. This requires a beam-training approach that accounts for subcarrier variations while maintaining low computational complexity. Let $\mu = \{\mu_1, \mu_2, \dots, \mu_L\}$ represent a predefined codebook of L candidate spatial directions. For each subcarrier m , the received signal y_m yields a received power p_m that can be computed as follows:

$$p_m = |y_m|^2. \quad (6)$$

Consequently, the objective is to estimate the proper UE spatial angle that maximizes the weighted sum of power measurements across the M subcarriers. The estimated UE's direction is given by:

$$\hat{\varsigma} = \arg \max_{\mu \in \mu} \sum_{m=1}^M w_m(\mu) \cdot p_m, \quad (7)$$

where $w_m(\mu)$ is a direction- and frequency-dependent weight related to subcarrier m . This formulation captures the trade-off between spatial resolution and robustness to beam-split.

To maintain analytical tractability in deriving the proposed beam training and interpolation strategy, we model the RIS with continuous-valued phase shifts. This assumption

enables closed-form analysis and clearer insight into the angular estimation process. However, we note that practical RIS hardware typically supports only finite-resolution phase quantization (e.g., 2-bit or 3-bit). To assess the impact of this discrepancy, Fig. 6 evaluates the achievable sum-rate under varying phase quantization levels. The results show that the proposed WBPC-AI method exhibits strong robustness, with only minor performance degradation even at low quantization resolutions. Thus, the continuous-phase assumption is justified as a reasonable upper-bound approximation and does not compromise the validity of the proposed method.

C. CONVENTIONAL ANALYTICAL BEAM TRAINING FRAMEWORK

A recent approach in [5] introduces a PDP-based analytical framework to estimate the user direction under the beam split effect. This method models the subcarrier-wise power behavior to refine the direction estimate. The estimation relies on the ratio of power measurements from two selected beam patterns, expressed as:

$$\zeta = \frac{p_1 - p_2}{p_1 + p_2}, \quad (8)$$

where p_1 and p_2 represent the measured powers of two probing beams centered at different candidate angles. Although this method improves direction estimation compared to conventional schemes, it has practical limitations. Reliance on a dominant beam pair makes it sensitive to alignment errors and measurement noise. Moreover, since the final direction is selected from a discrete codebook, resolution is limited, which can potentially lead to off-grid estimation errors. Signal quality also degrades at low SNRs, causing fluctuations and instability in the estimate. In the next section, we build on this insight to develop a more robust beam training strategy that reduces estimation variance and effectively mitigates the beam split effect in THz environments.

V. THE PROPOSED BEAM TRAINING FRAMEWORK WITH WBPC-AI

This section introduces our enhanced wideband beam training approach, termed WBPC-AI (Weighted Beam Pair Combination with Adaptive Interpolation), which improves the accuracy of direction estimation in RIS-assisted wideband THz systems. The proposed design extends the analytical PDP-based scheme in [5] by aggregating multi-beam responses and refining the output via local interpolation.

A. MOTIVATION AND KEY IDEAS

The baseline PDP-based method estimates the user direction $\hat{\varsigma}$ by analyzing the normalized power of a selected beam pair. However, selecting only the strongest beam pair introduces sensitivity to SNR and can lead to large estimation errors if the power peak is poorly defined. To address this issue, we propose the following enhancements:

- *Weighted Beam Pair Combination (WBPC)*: Instead of relying on a single beam pair, we adaptively combine multiple high-SNR beam pairs using an SNR-aware weighting scheme. This mitigates the outlier influence and smooths the PDP pattern. A detailed theoretical analysis of this mechanism is provided in Appendix A.
- *Adaptive Interpolation (AI)*: To achieve sub-codebook resolution, we locally interpolate around the most promising beams using a parametric model derived from adjacent received powers. This allows for precise refinement even with coarse beam codebooks. The mathematical analysis of this approach is given in Appendix B.

The parameter k that defines the number of top beams in WBPC is adaptively selected based on the SNR regime. In low SNR conditions, increasing k improves robustness by averaging out noise, whereas in high SNR conditions, a smaller k is sufficient for sharp estimation. In our simulations, we set $k = 3\text{--}5$ as a trade-off and discuss its impact in Section VI. Unlike the baseline PDP method in [5], which selects a single beam pair based on the peak PDP response (a hard decision), the proposed WBPC-AI framework:

- Combines *multiple* top- k beam responses using SNR-aware weighting to reduce susceptibility to noise and improve direction stability.
- Introduces interpolation to achieve sub-codebook resolution, whereas the baseline is limited by discrete codebook granularity.
- Maintains analytical simplicity with only marginal additional complexity of $\mathcal{O}(P \log k)$ over the baseline.

These enhancements enable WBPC-AI to outperform the PDP baseline, particularly in low-SNR or coarse-codebook regimes.

B. OVERVIEW OF THE PROPOSED WBPC-AI ALGORITHM

The beam training algorithm consists of three stages:

- 1) a training phase where power measurements are collected for each beam pair using the RIS codebook,
- 2) a weighted beam pair combination step that adaptively aggregates directional information from the top- k candidates based on SNR-aware weights, and
- 3) an interpolation-based refinement stage that enables sub-codebook resolution by estimating the actual direction from adjacent power responses.

Power normalization is essential to ensure fair comparison between beams with different widths and central angles. The normalization coefficients ζ are derived based on the beamwidth of each codeword, as explained in Appendix C.

The analytical formulation for constructing the codebook and normalizing the power is described in Appendix C. The algorithm achieves high estimation accuracy while maintaining low complexity and robustness to noise and quantization. Algorithm 1 presents the pseudocode for the proposed

Algorithm 1 WBPC-AI Beam Training Procedure

Inputs: Analytical codebook \mathcal{C} , central directions μ , subcarrier count M , normalization weights ζ .
Output: Estimated direction $\hat{\zeta}$

Require: RIS codebooks \mathcal{C} , direction centers μ , normalization factors ζ , number of subcarriers M , top- k value k

Ensure: Estimated user direction $\hat{\zeta}$

- 1: **Training Phase:**
- 2: **for** $i = 1$ to P **do** $\triangleright P$: total number of codewords
- 3: Configure RIS with beam pattern $\mathcal{C}[:, i]$
- 4: Transmit pilot signal, receive $p[i] = \sum_{m=1}^M |y_m^{(i)}|^2$
- 5: **end for**
- 6: Normalize power: $\tilde{p}[i] = p[i] \cdot \zeta[i]$
- 7: **Weighted Beam Combination (WBPC):**
- 8: Identify top- k beams: $\mathcal{I}_k = \arg \text{Top}_k(\tilde{p})$
- 9: **for** each $i \in \mathcal{I}_k$ **do**
- 10: Compute weight: $w[i] = \tilde{p}[i] / \sum_{j \in \mathcal{I}_k} \tilde{p}[j]$
- 11: **end for**
- 12: Compute weighted direction: $\mu_w = \sum_{i \in \mathcal{I}_k} w[i] \cdot \mu[i]$
- 13: **Interpolation-Based Refinement:**
- 14: Let $p_1 = \tilde{p}[i_1]$, $p_2 = \tilde{p}[i_2]$ be adjacent to μ_w
- 15: Compute ratio: $\chi = \frac{p_1 - p_2}{p_1 + p_2}$
- 16: Estimate refined direction:

$$\hat{\zeta} = \mu_w - \arcsin \left(\frac{\chi \sin(\Delta\mu) - \chi \sqrt{1 - \chi^2} \sin(\Delta\mu) \cos(\Delta\mu)}{\sin^2(\Delta\mu) + \chi^2 \cos^2(\Delta\mu)} \right)$$

WBPC-AI beam training procedure. Appendices A, B, and C provide a detailed analysis of each step in Algorithm 1.

C. COMPUTATIONAL COMPLEXITY

We analyze the computational complexity of the proposed WBPC-AI beam training framework under M subcarriers and a codebook of size P , and compare it with the baseline PDP-based analytical method [5] and existing beam training approaches in the literature.

The complexity of the WBPC-AI framework consists of three components. First, in the training stage, both the WBPC-AI and the baseline PDP-based methods perform P RIS configurations (beam pairs), each requiring power accumulation over M subcarriers. This results in a primary complexity of $\mathcal{O}(MP)$. Second, in the beam pair selection stage, WBPC-AI identifies the top- k beam pairs by partially sorting the normalized powers, incurring a complexity of $\mathcal{O}(P \log k)$. Third, the weighted beam combination and closed-form interpolation stages each require only a constant number of arithmetic operations, adding a negligible $\mathcal{O}(1)$ cost. Thus, the total computational complexity of the proposed WBPC-AI framework is as follows:

$$\mathcal{O}(MP + P \log k), \quad (9)$$

which introduces only a small additional overhead relative to the baseline PDP-based method that exploits beam split-induced power distribution patterns and operates at

TABLE 3. Computational complexity of beam training methods.

Method	Computational Complexity
Exhaustive Search [13]	$\mathcal{O}(MP)$
Hierarchical Search [14]	$\mathcal{O}(M \log P)$
Multi-Directional Q=2 [8]	$\mathcal{O}(2M)$
Multi-Directional Q=4 [8]	$\mathcal{O}(4M)$
PDP-Based Analytical [5]	$\mathcal{O}(MP)$
DNN (Training Phase) [17]	$\mathcal{O}(N_{\text{train}} \cdot d \cdot L)$
DNN (Inference Phase) [17]	$\mathcal{O}(d \cdot L^2)$
Enhanced Analytical (WBPC)	$\mathcal{O}(MP)$
Proposed WBPC-AI	$\mathcal{O}(MP + P \log k)$

a cost of $\mathcal{O}(MP)$ [5]. In return, WBPC-AI significantly improves the accuracy and robustness of the estimation in the presence of noise, codebook quantization, and beam split conditions, while maintaining scalability and low latency.

To contextualize this result, we compare WBPC-AI with other typical beam training approaches used in RIS-assisted wideband THz systems, including exhaustive search, hierarchical search, multi-directional training, and deep neural network (DNN)-based methods. The exhaustive search methods evaluate all possible beam directions using a full DFT codebook, resulting in a complexity of $\mathcal{O}(MP)$ but at the cost of significant delay [5]. Hierarchical search improves the efficiency to $\mathcal{O}(M \log P)$ by iteratively narrowing the search space into layers. While this method reduces training overhead, it requires feedback between layers and is less effective in multi-user or fast-varying channels. Multi-directional training schemes (e.g., using $Q = 2$ or $Q = 4$ wide beams) reduce training time to $\mathcal{O}(MQ)$ by probing multiple directions simultaneously [9]. Although this improves speed, these methods often suffer from reduced angular resolution and are especially vulnerable under beam-split conditions. DNN-based methods typically involve a complexity of $\mathcal{O}(d \cdot L^2)$, where d denotes the number of layers and L the number of neurons per layer [17]. Training such models incurs a high computational cost $\mathcal{O}(N_{\text{train}} \cdot d \cdot L)$, and their generalization performance can be degraded in deployment due to a mismatch with training conditions.

Table 3 summarizes the computational complexities and key trade-offs of these beam training methods. Compared to all other methods, the proposed WBPC-AI framework achieves an optimal balance of low complexity, scalability, and robustness, introducing only a minor $\mathcal{O}(P \log k)$ overhead while offering significant improvements in direction estimation performance across wideband and noisy scenarios.

VI. PERFORMANCE EVALUATION

A. SIMULATION SETUP

In this section, we evaluate the performance of the proposed WBPC-AI beam training framework through comprehensive simulations. The simulated RIS-assisted wideband THz communication system is configured with the following parameters: BS and UE are single-antenna devices, and the RIS is equipped with $N = \{512, 1024, 2048, 4096\}$ reflecting

elements. The carrier frequency is $f_c = 100$ GHz, the total bandwidth is $B = 10$ GHz, and the number of OFDM subcarriers is $M = 128$. The direction of the UE is drawn from a uniform distribution $\phi \sim \mathcal{U}(-\sqrt{3}/2, \sqrt{3}/2)$, as demonstrated in [5] for a fair comparison.

We assume a far-field planar wavefront, and elevation angle variation is neglected due to the assumed uniform user placement in the azimuthal plane. RIS phase shifts are modeled as $\phi_n = e^{j\theta_n}$ with θ_n drawn from a quantized phase set based on hardware resolution (e.g., 2-bit quantization). The channel is assumed reciprocal, and perfect synchronization is assumed across subcarriers.

The DNN baseline is implemented using a feedforward neural network with three hidden layers of sizes [128, 64, 32], ReLU activation, and a softmax output over the angular bins. The training dataset comprises 10,000 synthetic samples generated from randomized RIS channels with beam split effects. Training is performed using the Adam optimizer with a learning rate of 10^{-3} for 50 epochs and a mini-batch size of 128. This configuration is tuned for balanced performance and generalization.

We compare the performance of the proposed WBPC-AI framework with several benchmark schemes:

- Multi-directional beam training with $Q = 2$ and $Q = 4$ [9],
- DNN-based direction estimation [17],
- Conventional analytical PDP-based method [5],
- Exhaustive beam search (full-codebook scan), and
- Optimal beamforming (perfect direction knowledge), which serves as a performance upper bound.

All methods are evaluated under equal training overhead and identical codebook granularity.

Performance is assessed using three key metrics: (i) achievable rate (bps/Hz) under MRT-based beamforming with estimated DoA, (ii) mean squared error (MSE) of the angular estimation, and (iii) average runtime (in ms). Simulations are repeated over 1000 Monte Carlo trials per SNR to ensure statistical reliability.

B. SIMULATION RESULTS

Fig. 2 plots the achievable rate versus SNR across varying RIS sizes ($N = 512, 1024, 2048, 4096$) for the various methods. This figure reveals that increasing the RIS size leads to a consistent rate improvement for all schemes, due to the higher beamforming gain provided by the additional reflecting elements. It is clear that the proposed WBPC-AI method consistently delivers near-optimal performance and outperforms the other methods across all SNR levels and RIS sizes, demonstrating robustness and scalability. This is attributed to its dual-stage architecture, which combines a weighted beam pair for robustness against noise and interference, and an adaptive interpolation refinement mechanism that achieves sub-codebook resolution. The analytical PDP-based method also performs well, but lags behind the proposed framework, particularly for large RIS sizes. This

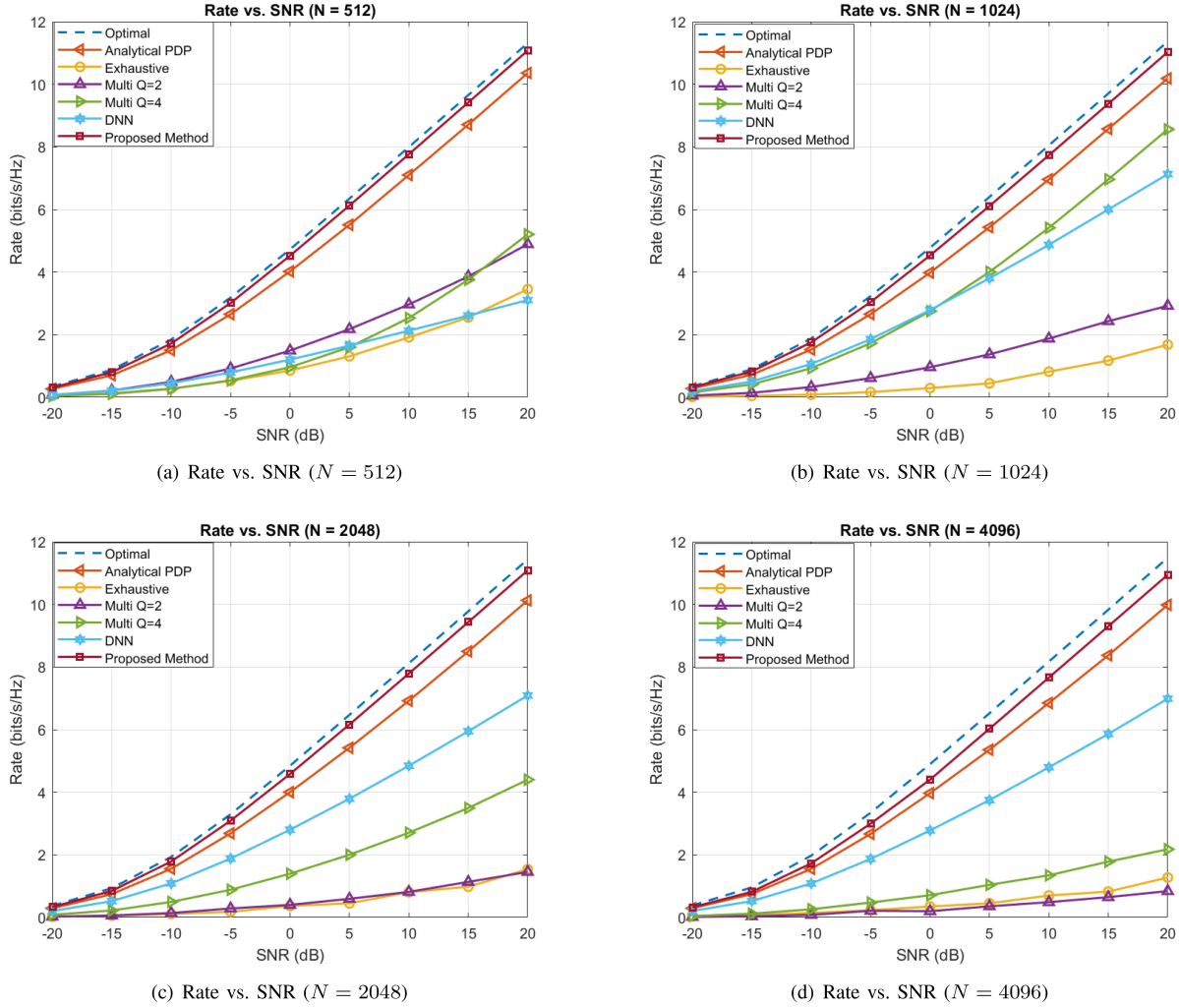


FIGURE 2. Achievable rate performance versus SNR for varying RIS sizes.

indicates the limitations of fixed codebooks and the lack of fine-angle resolution in PDP-based schemes. The gap between the proposed and analytical PDP methods widens with increasing N , highlighting the benefit of adaptivity in wideband and large-scale RIS scenarios. The multi-beam schemes with $Q = 2$ and $Q = 4$ perform significantly worse, especially at high SNR. Their inability to refine directional information results in early saturation, with minimal gain as the RIS scales. Similarly, the simulated DNN-based approach performs moderately, but does not scale well with N , due to its limited generalization and lack of structural knowledge embedded in the learning model. Interestingly, the exhaustive search method, often assumed to be a robust benchmark, performs poorly under these conditions. This is likely due to the impact of quantization errors and inefficient codebook coverage in high-dimensional angular spaces, which hinder its ability to exploit the available array gain. In general, the proposed WBPC-AI method demonstrates clear superiority in terms of rate performance, scalability with RIS size, and resilience to SNR variation.

Fig. 3 presents the achievable rate versus beam-training overhead for various methods, highlighting the critical trade-off between performance and training cost in RIS-assisted systems. The proposed WBPC-AI method achieves near-optimal performance with significantly lower overhead. In particular, it converges rapidly: beyond 128 training symbols, its performance approaches the optimal upper bound. This demonstrates the efficiency of weighted beam combination and adaptive refinement, which require only a limited number of beams to extract reliable channel information. In contrast, the PDP-based method converges more slowly and exhibits performance fluctuations at higher overhead levels because it relies on fixed beam patterns and lacks adaptive dynamic measurement. The exhaustive search method performs the worst across the entire range, reflecting its inefficiency in large search spaces and its vulnerability to quantization and noise. Multi-Q methods, particularly with $Q = 2$, require substantially more overhead to reach acceptable performance. Their fixed multi-beam patterns struggle to capture fine-grained directionality without excessive training. The DNN-based approach converges faster than Multi-Q

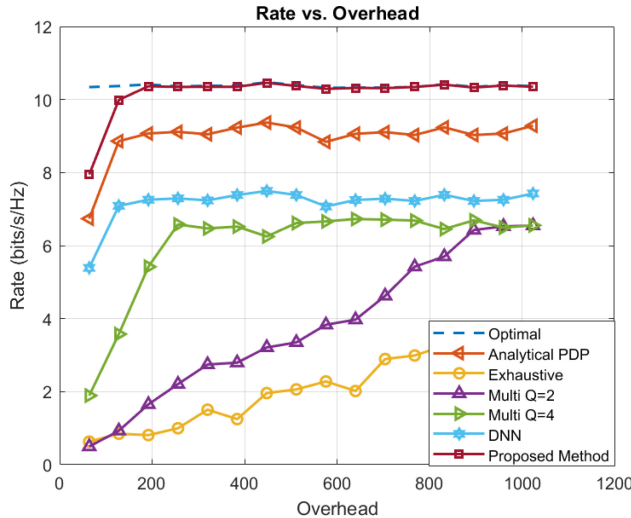


FIGURE 3. Achievable rate versus beam training overhead.

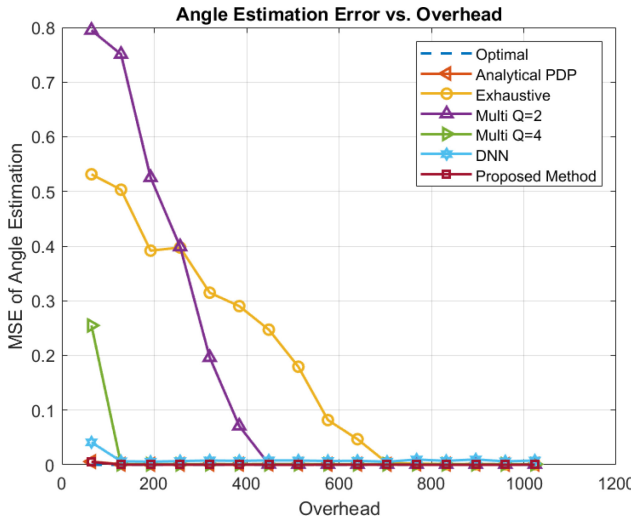


FIGURE 4. Angle estimation error (MSE) vs. beam training overhead for the various algorithms.

but saturates early, limited by the generalizability of the learning model. In general, Fig. 3 underscores the superiority of WBPC-AI in overhead efficiency. It is rapidly approaching optimal rate performance with minimal training, making it well-suited for real-time, low-latency RIS-assisted systems.

Fig. 4 illustrates the MSE of angle estimation as a function of beam-training overhead for various baseline methods. WBPC-AI exhibits slightly improved accuracy compared to the PDP method and outperforms other schemes. Notably, the multi-directional and exhaustive methods suffer from degraded resolution due to beam split, while WBPC-AI mitigates this through its effective weighted combination process.

Fig. 5 presents a comparative analysis of the proposed WBPC-AI method against several reference schemes under different RIS configurations: a uniform linear array (ULA) with $N = 2048$ and a UPA with 64×64 elements.

Figs. 5(a) and (b) show the rate performance versus SNR for the ULA and UPA setups, respectively, while Fig. 5(c) displays the average rate achieved by each method across configurations. As shown in Figs. 5(a) and (b), the proposed WBPC-AI method consistently achieves near-optimal rate performance throughout the SNR range for both RIS geometries. It outperforms all baseline methods. This gain is attributed to its two-stage architecture, which combines coarse angle estimation using weighted beam responses with adaptive fine-tuning. The UPA configuration offers slightly better performance than the ULA in high-SNR regions for most methods, primarily due to its 2D beamforming capability, which enhances spatial resolution and array gain. However, this benefit is not uniformly realized. Low-resolution approaches, such as Multi- $Q = 2/4$ and exhaustive search, still perform poorly, as they fail to exploit the additional spatial degrees of freedom available in the UPA. This contrast is further illustrated in Fig. 5(c), where the average rate of each method is compared across the two array configurations. The WBPC-AI method demonstrates strong scalability and generalization across different RIS geometries, maintaining near-optimal performance in both linear and planar array configurations.

Fig. 6 illustrates the impact of phase quantization on the achievable rate as a function of SNR for RIS systems of fixed size ($N = 1024$). Five quantization levels are considered, ranging from 1-bit to 5-bit resolution. The figure shows that increasing the number of quantization bits enhances performance, though the gains diminish beyond 3 bits. At low SNR, performance across all quantization levels is closely aligned, indicating that quantization noise has minimal impact in noise-limited regimes. As SNR increases, the performance gap widens, most notably between 1-bit and higher-resolution schemes. The 1-bit RIS suffers significant degradation due to insufficient phase resolution, which limits its ability to effectively align reflected signals. In contrast, 2-bit and 3-bit schemes closely approach the performance of 4-bit and 5-bit designs, especially in mid- to high-SNR regions. These results suggest that 3-bit quantization achieves a balanced trade-off between hardware complexity and rate performance, achieving near-optimal results with minimal cost. This finding supports the feasibility of low-resolution RIS implementations, particularly for large-scale deployments where hardware efficiency is critical.

Fig. 7 illustrates the average run-time of the various beam training methods under a fixed configuration of $N = 1024$ RIS elements and an SNR of 10 dB. This analysis highlights the computational complexity and practical feasibility of each technique in real-time deployment scenarios. The proposed WBPC-AI method achieves the lowest average runtime, significantly outperforming all baseline approaches in computational efficiency. It requires only a fraction of the runtime consumed by the exhaustive search method, which incurs the highest cost due to brute-force evaluation over the entire beam space, rendering it impractical for large-scale latency-sensitive systems. Multi-directional training

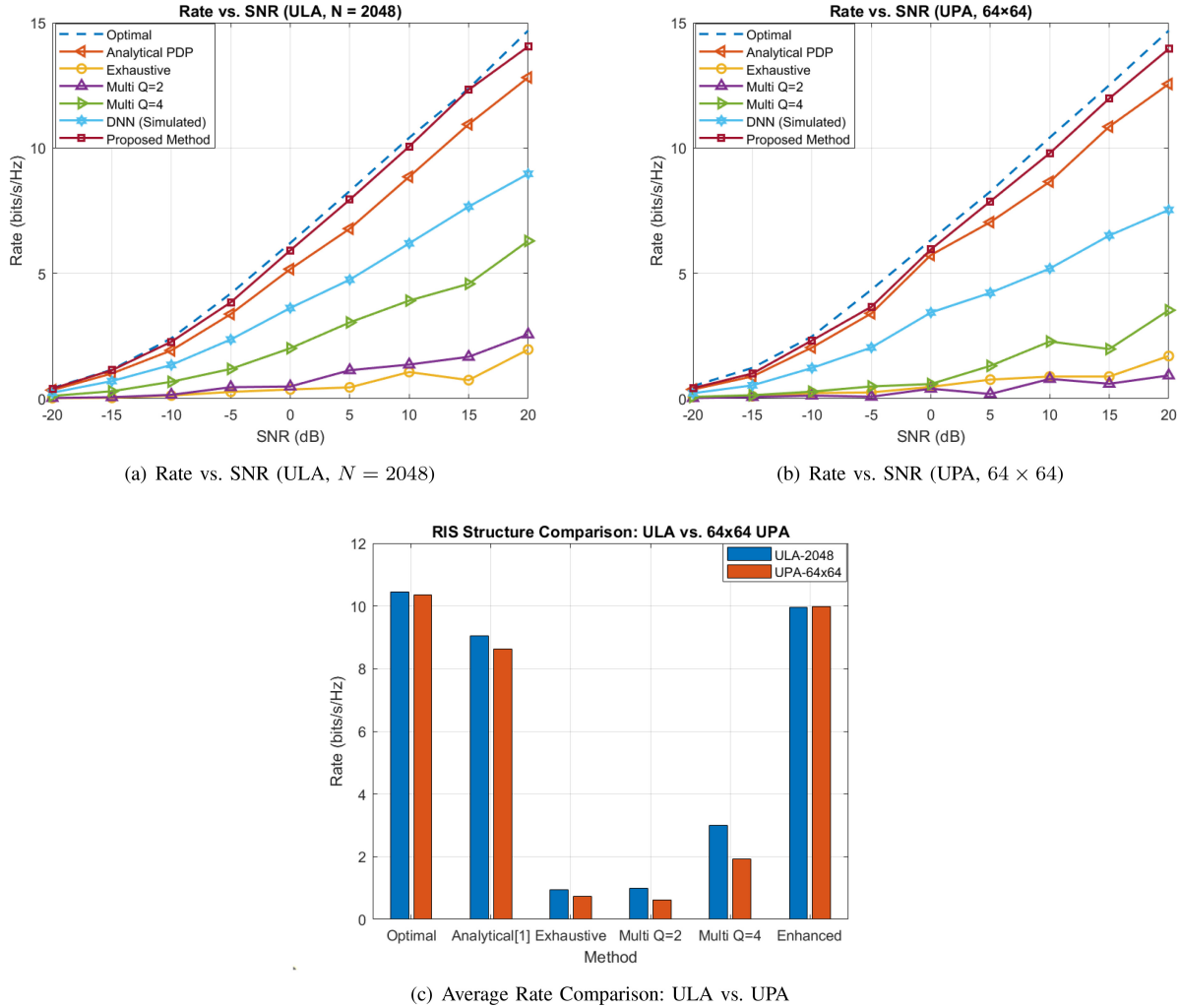


FIGURE 5. Comparison of achievable rate under ULA ($N = 2048$) and UPA (64×64) RIS structures for the various methods.

schemes ($Q = 2$ and $Q = 4$) also suffer from high runtime overhead, primarily due to repeated signal measurements across multiple directions without intelligent reuse or weighting. The analytical PDP-based method performs moderately, but is still limited by its fixed beam structure and lack of adaptive refinement, resulting in a processing cost higher than that of WBPC-AI. Interestingly, although not implementable in practice, the simulated Optimal method appears to have a low runtime in this comparison, as it bypasses estimation steps by assuming perfect channel knowledge. In contrast, WBPC-AI balances accuracy and efficiency by combining a lightweight weighted beam pair selection stage with a low-complexity refinement process. This hybrid approach significantly reduces computational cost without compromising estimation quality or achievable rate. These results confirm that the proposed method is both scalable and practical for real-time RIS-assisted systems.

To assess the performance and robustness of the proposed method, we simulate a RIS-assisted wideband THz communication system under ideal and hardware-impaired conditions. The system comprises $K = 4$ users, each served

via the RIS consisting of $N = 1024$ reflecting elements. The transmitter operates at a carrier frequency of $f_c = 0.1$ THz with a bandwidth of $B = 10$ GHz, divided into $num = 128$ subcarriers. Each user channel contains a single dominant path ($L = 1$), and RIS phase noise is modeled using a wrapped Gaussian distribution with a standard deviation of 5° to emulate realistic hardware imperfections.

Figure 8 illustrates the average sum-rate performance of five beam training methods evaluated in a multi-user ($K = 4$) THz system across an SNR range from -20 dB to 20 dB. Each method is evaluated under two conditions: clean RIS phase configuration (solid lines) and phase-noise-impaired RIS (dashed lines) with a standard deviation of $\sigma_\phi = 5^\circ$. The results show that the proposed WBPC-AI method consistently achieves the highest sum-rate across all SNR values and shows strong resistance to RIS phase noise. Although all baseline methods suffer some performance degradation under noisy conditions, WBPC-AI exhibits only a marginal rate loss, maintaining its superiority across the entire SNR range. Among the baseline schemes, the PDP-based method performs well but shows higher sensitivity

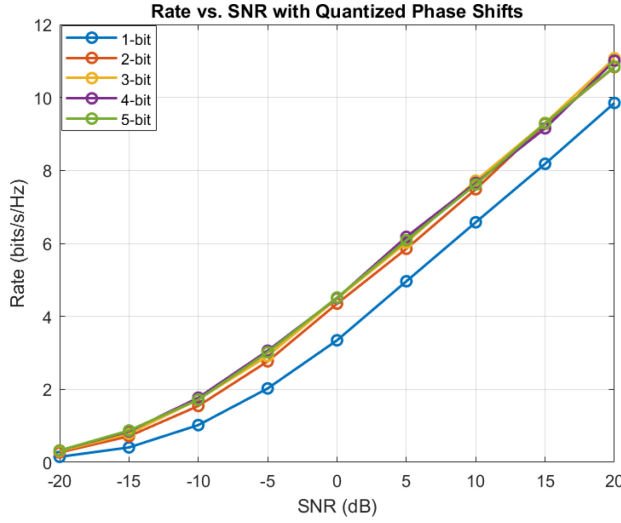


FIGURE 6. Achievable rate versus SNR for different phase quantization levels of the RIS elements with 1024 RIS elements.

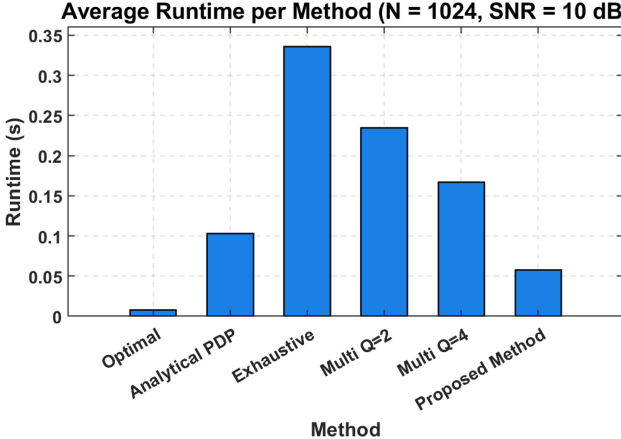


FIGURE 7. Average runtime per method at $N = 1024$ and $\text{SNR} = 10 \text{ dB}$.

to phase noise, particularly at high SNR. Multi-directional methods (Multi-Q2 and Multi-Q4) exhibit moderate robustness depending on beamwidth configuration, with Multi-Q4 outperforming Multi-Q2 due to its narrower beam alignment. In contrast, the exhaustive search method yields the lowest performance in both clean and noisy scenarios due to coarse resolution and large overhead, making it impractical for real-time deployment. These findings highlight the efficiency, robustness, and practical deployment of the proposed WBPC-AI framework for RIS-assisted THz systems. Unlike data-driven solutions such as DNN-based approaches, which often degrade dramatically under hardware impairments and lack generalization, the WBPC-AI scheme maintains high performance in ideal and hardware-impaired environments.

Figure 9 illustrates the average achievable rate performance of six beam training methods as the number of users increases from 4 to 16, under ideal RIS conditions (i.e., without phase noise). The SNR is fixed at 10 dB, and each curve represents the average of 100 Monte Carlo

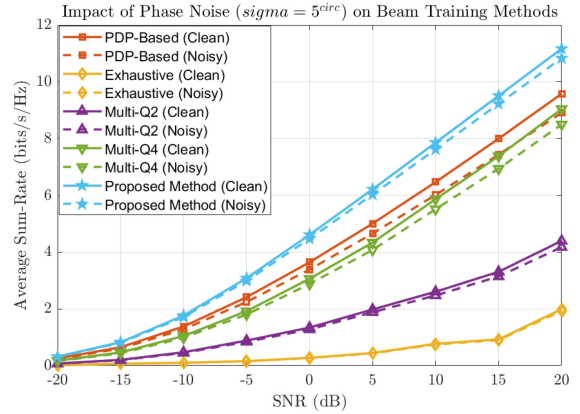


FIGURE 8. Comparison of average sum-rate performance for five beam training methods under a multi-user ($K = 4$) THz system with and without RIS phase noise ($\sigma_\phi = 5^\circ$).

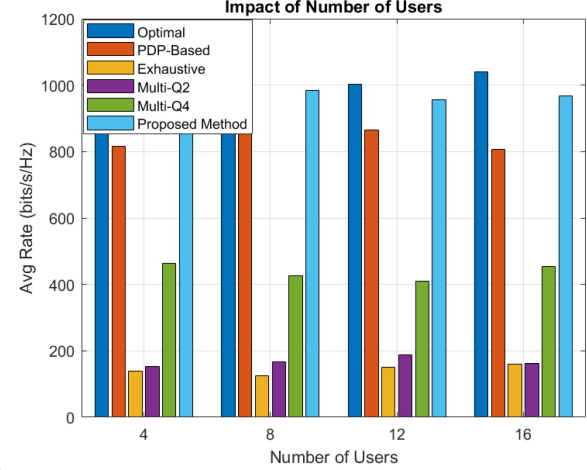


FIGURE 9. Average rate performance of six beam training methods vs. number of users under clean RIS configuration (no phase noise, $\text{SNR} = 10 \text{ dB}$, 100 Monte Carlo trials).

realizations. The Optimal and proposed WBPC-AI methods consistently achieve the highest performance across all user counts. In particular, the proposed method closely aligns with the Optimal baseline, validating its efficiency under clean conditions. The PDP-based approach performs well for small user counts, but degrades more significantly as the number of users increases, likely due to the limitations of path-based estimation when multi-user interference increases.

Multi-Q2 and Multi-Q4 strategies show moderate scalability; however, Multi-Q4 maintains a better rate due to improved beam resolution. The Exhaustive method consistently indicates poor performance, highlighting its inefficiency and resolution limitations, especially when scaled to larger user counts. These findings reinforce that while optimal solutions are ideal under clean assumptions, the Proposed Method provides a robust and scalable alternative suitable for practical multi-user RIS-assisted THz systems.

Table 4 summarizes the qualitative performance of the evaluated beam training methods across three key criteria:

TABLE 4. Qualitative comparison of beam training methods.

Method	Estimation Accuracy	Robustness (Low SNR)	Sub-Codebook Resolution
Exhaustive Search [13]	High	Low	No
Hierarchical Search [14]	Medium	Low	No
Multi Q=2	Low-Medium	Low	No
Multi Q=4	Medium	Medium	No
PDP-Based Analytical [5]	Medium-High	Medium	No
DNN [17]	Medium	Medium	Yes
Enhanced Analytical (WBPC)	High	High	Partial
Proposed WBPC-AI	High	High	Yes

estimation accuracy, robustness under low SNR, and support for sub-codebook resolution. Exhaustive search achieves high accuracy through brute-force evaluation, but is computationally expensive and sensitive to noise. Hierarchical and multi-beam methods offer low complexity, but suffer from limited resolution and poor performance in low-SNR conditions. The analytical PDP-based method enhances the estimation via delay-phase matching but is limited by codebook granularity. DNN-based approaches offer moderate robustness and flexibility, but they heavily depend on generalization during training. In contrast, the proposed WBPC-AI method combines high accuracy, strong low-SNR robustness, and sub-codebook resolution through adaptive refinement, offering an effective trade-off between precision, complexity, and practical deployment.

Compared to the PDP-based baseline [5], the proposed WBPC-AI framework achieves notable improvements across all key metrics. First, WBPC-AI exhibits higher estimation accuracy by combining multiple beam responses with SNR-aware weighting, which mitigates the vulnerability of single-beam selection under noise. Second, it introduces sub-codebook resolution through an interpolation-based refinement stage, enabling more precise direction estimation beyond the limitations of coarse codebooks. Third, WBPC-AI shows stronger robustness in low-SNR environments, where PDP-based methods suffer from quantization and decision errors. Finally, the proposed method maintains low complexity and significantly lower runtime, scaling efficiently with RIS size and supporting both ULA and UPA configurations. These enhancements make WBPC-AI a practical and superior alternative to existing analytical beam training approaches.

VII. CONCLUSION

This work presented an efficient and robust beam training framework for RIS-assisted wideband THz communication systems, referred to as WBPC-AI. The proposed method builds upon the foundation of the analytical power-delay profile (PDP)-based technique, introducing two key enhancements to address the unique challenges of THz communication. First, the weighted beam pair combination (WBPC) mechanism aggregates directional energy from multiple high-SNR beam pairs, improving resilience to adverse conditions such as low SNR and sparse training overhead. Second, the AI step enables sub-codebook resolution, mitigating angular quantization errors typically caused by coarse beamforming codebooks. WBPC-AI retains the computational efficiency of the original PDP-based method while overcoming the limitations associated with THz frequencies,

such as spatial-wideband beam-split effects. By integrating these enhancements, the framework achieves improved angle estimation accuracy and achievable rate performance, particularly in complex THz environments. Simulation results demonstrated that WBPC-AI consistently outperforms existing beam training methods, including exhaustive search, hierarchical training, multi-beam approaches, deep learning-based schemes, and the baseline PDP-based estimator. The robustness of the proposed framework was further validated under low-bit quantization (1-bit and 2-bit phase quantization), confirming its suitability for practical RIS-assisted THz communication systems. Additionally, the proposed method seamlessly extends to RIS configurations for uniform linear arrays and UPA, making it versatile for various deployment scenarios. This work sets the stage for more efficient and reliable beam training in next-generation THz communication systems, offering substantial improvements in performance and computational efficiency.

APPENDIX A DERIVATION OF WEIGHTED BEAM PAIR COMBINATION (WBPC)

In the proposed WBPC-AI framework, instead of selecting a single beam pair with the highest normalized power, we aggregate multiple top- k beam pairs based on their received powers. This strategy enhances robustness in noisy environments by mitigating the sensitivity to any single suboptimal beam pair.

Let $p[i]$ denote the accumulated received power for the i -th beam pair across all subcarriers:

$$p[i] = \sum_{m=1}^M |y_m^{(i)}|^2. \quad (10)$$

To ensure fairness among beams with different angular widths, we normalize the received power using a beam-dependent factor $\zeta[i]$ derived from the codebook structure:

$$\tilde{p}[i] = p[i] \cdot \zeta[i]. \quad (11)$$

Next, we select the index set \mathcal{I}_k corresponding to the top- k beams with the highest normalized power values. The weight assigned to each selected beam is proportional to its normalized energy:

$$w[i] = \frac{\tilde{p}[i]}{\sum_{j \in \mathcal{I}_k} \tilde{p}[j]}, \quad \forall i \in \mathcal{I}_k. \quad (12)$$

The final estimated coarse direction μ_w is then calculated as the weighted average of the central directions of the selected beams:

$$\mu_w = \sum_{i \in \mathcal{I}_k} w[i] \cdot \mu[i]. \quad (13)$$

This aggregation process improves stability compared to hard decision methods by smoothing out noisy fluctuations in the power-delay profile. In addition, it enables for more accurate refinement in the subsequent interpolation step.

The WBPC stage introduces negligible additional complexity since $k \ll P$, and all operations are linear in k .

In our implementation, we use a fixed $k = 3$ unless otherwise noted, as it was empirically found to balance robustness and directional resolution under various SNR and codebook configurations.

The adaptive interpolation step in WBPC-AI estimates the dominant AoA $\hat{\theta}$ within a given beam sector using a weighted combination of pre-computed power measurements at discrete grid points. Given three adjacent steering directions $\{\theta_{i-1}, \theta_i, \theta_{i+1}\}$ and their corresponding received powers $\{P_{i-1}, P_i, P_{i+1}\}$, a convex quadratic fit obtains the estimated direction:

$$\hat{\theta} = \theta_i + \frac{\Delta}{2} \cdot \frac{P_{i-1} - P_{i+1}}{P_{i-1} - 2P_i + P_{i+1}},$$

where Δ denotes the grid spacing. This interpolation model assumes a smooth angular variation in received power and is resilient to moderate phase distortions because it relies on relative power trends rather than absolute values. To evaluate robustness under phase noise, we simulate a wrapped Gaussian-distributed perturbation with $\sigma_\phi = 5^\circ$ applied to the RIS phases. As shown in Fig. 8, the proposed interpolation-based estimation exhibits minimal degradation, confirming that the estimated AoA remains accurate even with distorted phase responses. This robustness stems from the use of narrowband energy peaks and redundant power aggregation over codebook beams, which naturally suppresses random phase fluctuation effects. The convex interpolation avoids overfitting to noisy measurements, which enhances stability.

APPENDIX B DERIVATION OF AI-BASED DIRECTION ESTIMATION

After computing the weighted center μ_w in the WBPC stage, we refine the user's direction estimate using a parametric interpolation scheme based on the power profile of the adjacent beams. Let p_1 and p_2 denote the normalized powers of the two beam pairs centered at $\mu_w - \delta$ and $\mu_w + \delta$, respectively.

We define the ratio metric χ as:

$$\chi = \frac{p_1 - p_2}{p_1 + p_2}. \quad (14)$$

This metric encodes the relative steepness of the power profile around the peak, and under symmetry assumptions, $\chi = 0$ corresponds to the peak being exactly at μ_w . A positive (negative) χ implies that the peak is shifted toward the left (right) neighbor, motivating a corrective adjustment.

To better illustrate the refinement process, Fig. 10 visualizes the direction estimation correction based on the power asymmetry between two adjacent beams. The estimated offset from the central beam μ is guided by the ratio metric χ in (14), enabling a sub-codebook resolution interpolation using p_1 and p_2 .

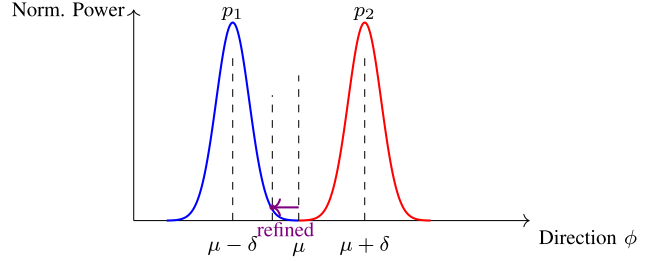


FIGURE 10. Direction refinement via interpolation using adjacent beam powers p_1 and p_2 . The offset from μ is based on χ in (14).

We assume that the power profile $p(\phi)$ around a central beam direction μ follows a normalized idealized pattern derived from the array factor:

$$p(\phi) \propto \frac{\sin^2\left(\frac{\pi N_s(\phi-\mu)}{2}\right)}{\sin^2\left(\frac{\pi(\phi-\mu)}{2}\right)}, \quad (15)$$

where N_s is the effective number of subcarriers that contribute to the beamforming gain.

Using this model, we can analytically relate the power ratio χ to the offset of the true DoA from μ_w . By inverting the power asymmetry between adjacent beams, we derive a refined estimate $\hat{\phi}$ for the direction of arrival as:

$$\begin{aligned} \hat{\phi} &= \mu_w \\ &- \arcsin\left(\frac{\chi \sin(\pi\delta) - \chi \sqrt{1 - \chi^2} \sin(\pi\delta) \cos(\pi\delta)}{\sin^2(\pi\delta) + \chi^2 \cos^2(\pi\delta)}\right). \end{aligned} \quad (16)$$

This closed-form expression offers a low-complexity refinement and is robust to noise and quantization effects. The derivation assumes a narrow angular region around μ_w where the approximation holds, and it is especially effective when the codebook is coarse but symmetric.

Given the top 2-beam powers p_1 and p_2 associated with their respective angles θ_1 and θ_2 , the refined direction estimate θ_{refined} is computed using a linear interpolation scheme based on power asymmetry. Specifically,

$$\theta_{\text{refined}} = \theta_1 + \alpha(\theta_2 - \theta_1), \quad \text{where } \alpha = \frac{p_2}{p_1 + p_2}. \quad (17)$$

This interpolation reflects the intuition that the stronger beam (higher p) pulls the estimated angle closer to its direction. The interpolation provides sub-codebook resolution with negligible additional complexity.

Interpolation Accuracy Bound: Assuming a smooth power profile $p(\phi)$ and symmetric beam spacing, the maximum estimation error of the interpolated angle is bounded by:

$$|\theta_{\text{refined}} - \theta^*| \leq \frac{\Delta}{2} \cdot \left| \frac{p_1 - p_2}{p_1 + p_2} \right|, \quad (18)$$

where $\Delta = |\theta_2 - \theta_1|$ and θ^* is the true AoA. This bound confirms that as the power asymmetry decreases (i.e., when $p_1 \approx p_2$), the error becomes negligible.

Complexity Analysis: The computational cost of this interpolation refinement is $\mathcal{O}(1)$ per beam pair, involving only a few arithmetic operations and a trigonometric function. Compared to grid search complexity of $\mathcal{O}(N)$ or matched filtering with $\mathcal{O}(N \log N)$, this method adds negligible overhead, making it suitable for real-time applications.

Proposition: Under mild smoothness assumptions on the power profile and sufficient beam overlap, the refined angle θ_{refined} achieves sub-grid resolution with mean squared error (MSE) decreasing as $\mathcal{O}(\Delta^2)$, thereby outperforming hard-decision beam selection. This interpolation mechanism enables sub-codebook resolution by estimating the PDP peak between discrete directions, allowing WBPC-AI to outperform hard-decision schemes that are limited to the predefined grid of μ .

APPENDIX C ANALYTICAL CODEBOOK AND NORMALIZATION COEFFICIENTS

The WBPC-AI method requires the construction of an angular codebook and a corresponding set of normalization coefficients to ensure fairness across different beam patterns.

Let $\mu = \{\mu[1], \mu[2], \dots, \mu[P]\}$ denote the central angles of P codewords, uniformly spaced in the angular domain $[-1, 1]$. Each beam pair in the codebook is defined with a symmetric beam width of 2δ , such that:

$$\mu[i] = -1 + (2i - 1)\delta, \quad \text{for } i = 1, 2, \dots, P, \quad (19)$$

where $\delta = 1/P$ defines the half-width between neighboring beams.

The codebook spacing 2δ ensures uniform angular coverage while allowing beam overlap. This is critical for both accurate direction estimation and smooth interpolation in later stages.

To avoid edge effects during interpolation, each beam's usable range is limited to:

$$[\mu[i] - \kappa\delta, \mu[i] + \kappa\delta], \quad (20)$$

where $\kappa \in (0, 1)$ is a tunable parameter that controls overlap and the confidence range around each central angle. Since different beams may contribute varying amounts of energy due to their beamwidths, normalization is necessary to prevent selection bias during WBPC.

We define the power normalization coefficient $\zeta[i]$ for each beam based on its effective width:

$$\zeta[i] = \frac{2\delta_i}{\sum_{j=1}^P 2\delta_j} = \frac{\delta_i}{\sum_{j=1}^P \delta_j}. \quad (21)$$

For uniformly spaced beams, $\delta_i = \delta$ for all i , which leads to a uniform normalization factor: $\zeta[i] = \frac{1}{P}$. However, in general or adaptive codebooks, beam widths may vary slightly due to shaping or grid optimization, making this normalization essential.

After collecting raw beam power measurements $p[i]$, the normalized values are computed as:

$$\tilde{p}[i] = p[i] \cdot \zeta[i]. \quad (22)$$

These normalized powers are used in both the top- k selection and the WBPC aggregation, ensuring that beam pairs with different spatial spreads are treated equitably. This design allows the WBPC-AI method to operate robustly even when the codebook granularity is coarse, and it maintains fairness when combining beams with unequal angular contributions.

ACKNOWLEDGMENT

The authors gratefully acknowledge the Research Office at UAEU for funding the article processing charges (APC) of this publication.

REFERENCES

- [1] M. Al-Quraan et al., "Enhancing reliability in federated mmWave networks: A practical and scalable solution using radar-aided dynamic blockage recognition," *IEEE Trans. Mobile Comput.*, vol. 23, no. 10, pp. 10146–10160, Oct. 2024.
- [2] P. Singh, H. B. Salameh, V. A. Bohara, A. Srivastava, and M. Ayyash, "Jamming-resilient mirror element allocation scheme for OIRS-aided UAV-based FSO networks," *IEEE Trans. Intell. Veh.*, early access, Aug. 26, 2024, doi: [10.1109/TIV.2024.3450191](https://doi.org/10.1109/TIV.2024.3450191).
- [3] H. Al-Obiedollah, H. B. Salameh, A. M. Hayajneh, and S. A. R. Zaidi, "Throughput-fairness trade-off optimization for IRS NOMA systems," *IEEE Access*, early access, Jan. 28, 2025, doi: [10.1109/ACCESS.2025.3535839](https://doi.org/10.1109/ACCESS.2025.3535839).
- [4] H. B. Salameh, H. Al-Obiedollah, Y. Jararweh, W. abu Eid, and S. Abdel-Razeq, "Adaptive power optimization in IRS-assisted hybrid OFDMA-NOMA cognitive radio networks with dynamic TDMA slot allocation," *Ad Hoc Netw.*, vol. 170, Apr. 2025, Art. no. 103778.
- [5] Y. Chen, J. Tan, M. Hao, R. MacKenzie, and L. Dai, "Accurate beam training for RIS-assisted wideband terahertz communication," *IEEE Trans. Commun.*, vol. 71, no. 12, pp. 7425–7440, Dec. 2023.
- [6] Q. Wu and R. Zhang, "Intelligent reflecting surface enhanced wireless network via joint active and passive beamforming," *IEEE Trans. Wireless Commun.*, vol. 18, no. 11, pp. 5394–5409, Nov. 2019.
- [7] C. Huang et al., "Multi-hop RIS-empowered terahertz communications: A DRL-based hybrid beamforming design," *IEEE J. Sel. Areas Commun.*, vol. 39, no. 6, pp. 1663–1677, Jun. 2021.
- [8] C. You, B. Zheng, and R. Zhang, "Fast beam training for IRS-assisted multi-user communications," *IEEE Wireless Commun. Lett.*, vol. 9, no. 11, pp. 1845–1849, Nov. 2020.
- [9] P. Wang, J. Fang, W. Zhang, and H. Li, "Fast beam training and alignment for IRS-assisted millimeter wave/terahertz systems," *IEEE Trans. Wireless Commun.*, vol. 21, no. 4, pp. 2710–2724, Apr. 2022.
- [10] L. Dai et al., "Reconfigurable intelligent surface-based wireless communications: Antenna design, prototyping, and experimental results," *IEEE Access*, vol. 8, pp. 45913–45923, 2020.
- [11] X. Gao, L. Dai, Z. Chen, Z. Wang, and Z. Zhang, "Near-optimal beam selection for beamspace mmWave massive MIMO systems," *IEEE Commun. Lett.*, vol. 20, no. 5, pp. 1054–1057, May 2016.
- [12] R. Piesiewicz et al., "Short-range ultra-broadband terahertz communications: Concepts and perspectives," *IEEE Antennas Propag. Mag.*, vol. 49, no. 6, pp. 24–39, Dec. 2007.
- [13] J. Wang et al., "Beam codebook based beamforming protocol for multi-Gbps millimeter-wave WPAN systems," *IEEE J. Sel. Areas Commun.*, vol. 27, no. 8, pp. 1390–1399, Oct. 2009.
- [14] Z. Xiao, T. He, P. Xia, and X.-G. Xia, "Hierarchical codebook design for beamforming training in millimeter-wave communication," *IEEE Trans. Wireless Commun.*, vol. 15, no. 5, pp. 3380–3392, May 2016.
- [15] H. Yu et al., "An improved beam training scheme under hierarchical codebook," *IEEE Access*, vol. 8, pp. 53627–53635, 2020.
- [16] B. Ning et al., "Terahertz multi-user massive MIMO with IRS: Beam training and hybrid beamforming," *IEEE Trans. Veh. Technol.*, vol. 70, no. 2, pp. 1376–1393, Feb. 2021.
- [17] C. Qi et al., "Deep learning for beam training in millimeter wave massive MIMO systems," *IEEE Trans. Wireless Commun.*, early access, Sep. 22, 2020, doi: [10.1109/TWC.2020.3024279](https://doi.org/10.1109/TWC.2020.3024279).

- [18] Z. Albataineh, "Reducing pilot overhead with distributed neural networks in RIS-aided downlink channel estimation," *Results Eng.*, vol. 26, Jun. 2025, Art. no. 105036, doi: [10.1016/j.rineng.2025.105036](https://doi.org/10.1016/j.rineng.2025.105036).
- [19] Z. Albataineh, M. A. Bataineh, K. F. Hayajneh, and R. A. Athamneh, "Advanced 5G channel estimation in mmWave MIMO systems: Leveraging compressive sensing for enhanced performance," *IEEE Access*, vol. 13, pp. 72104–72115, 2025, doi: [10.1109/ACCESS.2025.3560829](https://doi.org/10.1109/ACCESS.2025.3560829).
- [20] W. Liu et al., "Low-overhead beam training for extremely large-scale RIS," *IEEE Trans. Commun.*, vol. 71, no. 8, pp. 4924–4940, Aug. 2023.
- [21] X. Mo et al., "Beamspace channel estimation with beam squint effect for mmWave MIMO-OFDM," *IEEE Access*, vol. 9, pp. 153037–153049, 2021.
- [22] J. Tan and L. Dai, "Delay-phase precoding for THz massive MIMO with beam split," in *Proc. IEEE GLOBECOM*, Dec. 2019, pp. 1–6.
- [23] Y. Chen and L. Dai, "Coded beam training for RIS assisted wireless communications," *IEEE Trans. Wireless Commun.*, vol. 24, no. 5, pp. 3854–3867, May 2025.
- [24] A. N. Taha, Y. E. Elghaib, and A. Alkhateeb, "Enabling large intelligent surfaces with compressive sensing and deep learning," *IEEE Access*, vol. 9, pp. 44304–44321, 2021.
- [25] C. Pan et al., "Multicell MIMO communications relying on intelligent reflecting surfaces," *IEEE Trans. Wireless Commun.*, vol. 19, no. 8, pp. 5218–5233, Aug. 2020.
- [26] Y. Pan, C. Pan, S. Jin, and J. Wang, "RIS-aided near-field localization and channel estimation for the terahertz system," *IEEE J. Sel. Topics Signal Process.*, vol. 17, no. 4, pp. 878–892, Jul. 2023.
- [27] A. Simoncic, P. Pevec, and T. Javornik, "Near-field beam steering with planar antenna array for THz systems," 2024, *arXiv:2403.06789*.
- [28] R. Long, Y. Zeng, and R. Zhang, "Active reconfigurable intelligent surface-aided wireless communications," *IEEE Trans. Wireless Commun.*, vol. 20, no. 8, pp. 4962–4975, Aug. 2021.
- [29] Z. Albataineh, H. B. Salameh, and M. Al Bataineh, "Two-stage power allocation for IRS-assisted Downlink NOMA: Intra-group optimization and inter-group allocation," *IEEE Access*, vol. 13, pp. 90052–90062, 2025.



ZAID ALBATAINEH (Senior Member, IEEE) received the Ph.D. degree in electrical and computer engineering from Michigan State University, East Lansing, MI, USA. He is currently a Professor with the Department of Electronics Engineering, Yarmouk University, Irbid, Jordan, where he also serves as a Vice Dean with the Hijjawi Faculty for Engineering Technology. From 2019 to 2024, he was the Head of the Electronics Engineering Department and previously held the position of Acting Dean. He has published extensively in IEEE and Elsevier journals and supervises numerous undergraduate and graduate projects in communications, AI, and embedded systems. His research interests include millimeter-wave massive MIMO, reconfigurable intelligent surfaces, NOMA systems, hybrid metaheuristic optimization, and machine learning for wireless communication.



HAYTHEM BANY SALAMEH (Senior Member, IEEE) received the Ph.D. degree in electrical and computer engineering from the University of Arizona, Tucson, AZ, USA, in 2009. He is currently a Professor of communications and networking engineering with Al Ain University, Al Ain, UAE (on leave from Yarmouk University (YU), Irbid, Jordan). He is the Dean of the Graduate Studies and Scientific Research, Al Ain University. He also holds a Visiting Professor position with Staffordshire University, Stoke-on-Trent, U.K. His research interests include wireless networking, emphasizing dynamic spectrum access, cognitive radio networking, Internet of Things, security, and distributed protocol design. He was a recipient of the Jordan Science Research Support Foundation (SRSF) Prestigious Award for Distinguished Research in ICT in 2015, the Best Researcher Award for Scientific Colleges in YU in 2016, and the SRSF Award for Creativity and Technological Scientific Innovation in 2017. He has served and continues to serve on the Technical Program Committee of many international conferences.



MOHAMMAD AL BATAINEH received the B.S. degree (Hons.) in telecommunications engineering from Yarmouk University, Jordan, in 2003, and the M.S. and Ph.D. degrees in electrical engineering from the Illinois Institute of Technology, USA, in 2006 and 2010, respectively. Subsequent to his academic pursuits, he held noteworthy positions at institutions, including Yarmouk University, where he was promoted to an Associate Professor, in 2018, and roles with Argonne National Laboratories and MicroSun Technologies. In August 2020, he joined as an Assistant Professor with United Arab Emirates University. His research interests include the application of communications, coding theory, and information theory to the interpretation and understanding of information flow in biological systems, particularly gene expression. His additional research avenues encompass machine learning, network information theory, and optimization.



AHMED MUSA ALSHORMAN received the Ph.D. degree in electrical engineering from the University of Texas at El Paso, TX, USA, in 2006. He is currently a Professor of communication engineering with the Hijjawi Faculty for Engineering Technology, Yarmouk University, Irbid, Jordan. He previously served as a Vice Dean and the Head of the Communication Engineering Department, Al-Hussein Bin Talal University, Ma'an, Jordan. His research interests include telecommunication networks, wireless and optical communications, data compression, and network optimization.